JOURNAL OF VIROLOGY, Oct. 1996, p. 7039–7048
0022-538X/96/$04.00+0

Vol. 70, No. 10

Analysis of the VPg-Proteinase (NIa) Encoded by Tobacco Etch Potyvirus: Effects of Mutations on Subcellular Transport, Proteolytic Processing, and Genome Amplification

MARY C. SCHAAD, RUTH HALDEMAN-CAHILL, STEPHEN CRONIN, AND JAMES C. CARRINGTON*

Department of Biology, Texas A&M University, College Station, Texas 77843

Received 20 February 1996/Accepted 19 June 1996

A mutational analysis was conducted to investigate the functions of the tobacco etch potyvirus VPg-proteinase (NIa) protein in vivo. The NIa N-terminal domain contains the VPg attachment site, whereas the C-terminal domain contains a picornavirus 3C-like proteinase. Cleavage at an internal site separating the two domains occurs in a subset of NIa molecules. The majority of NIa molecules in TEV-infected cells accumulate within the nucleus. By using a reporter fusion strategy, the NIa nuclear localization signal was mapped to a sequence within amino acid residues 40 to 49 in the VPg domain. Mutations resulting in debilitation of NIa nuclear translocation also debilitated genome amplification, suggesting that the NLS overlaps a region critical for RNA replication. The internal cleavage site was shown to be a poor substrate for NIa proteolysis because of a suboptimal sequence context around the scissile bond. Mutants that encoded NIa variants with accelerated internal proteolysis exhibited genome amplification defects, supporting the hypothesis that slow internal processing provides a regulatory function. Mutations affecting the VPg attachment site and proteinase active-site residues resulted in amplification-defective viruses. A transgenic complementation assay was used to test whether NIa supplied in *trans* could rescue amplification-defective viral genomes encoding altered NIa proteins. Neither cells expressing NIa alone nor cells expressing a series of NIa-containing polyproteins supported increased levels of amplification of the mutants. The lack of complementation of NIa-defective mutants is in contrast to previous results obtained with RNA polymerase (NIb)-defective mutants, which were relatively efficiently rescued in the transgenic complementation assay. It is suggested that, unlike NIb polymerase, NIa provides replicative functions that are *cis* preferential.

Tobacco etch virus (TEV) is a well-characterized member of the *Potyviridae*, a family belonging to the picornavirus supergroup of RNA plus-stranded viruses (27). It possesses a genome that is linked covalently to a protein (VPg) and that encodes a large polyprotein that is proteolytically processed by three virus-encoded proteinases (17, 36). The P1 and HC-Pro proteinases catalyze autoproteolytic cleavages within the N-terminal region of the polyprotein (7, 42). A third TEV proteinase, NIa, resembles the picornavirus 3C proteinase and catalyzes *cis*- and *trans*-proteolytic reactions within the C-terminal two-thirds of the polyprotein (6, 8, 9, 16, 18, 21). The 3C-like proteinases contain a polypeptide fold resembling chymotrypsin, but with a cysteine rather than serine occupying the nucleophilic position within the active site (1, 5, 20, 26).

The NIa protein is actually a polyprotein consisting of a C-terminal proteinase domain and an N-terminal VPg domain. The domains are separated by an internal cleavage site recognized by NIa (16). The context of this site deviates from the consensus heptapeptide sequence motif that characterizes each of the other NIa cleavage sites, providing a possible explanation for the inefficient processing observed at this site in vivo and in vitro (13, 16). Despite its slow cleavage kinetics, the internal cleavage site appears to be essential for RNA amplification, as a mutation that abolishes internal processing renders the genome nonviable (13). The VPg attaches covalently to the 5′ terminus of genomic RNA through a phosphodiester linkage with the hydroxyl group of Tyr-62 (28, 29, 38). In fact, both full-length NIa (49 kDa) and the processed VPg domain (21 kDa) have been detected among the products released from genomic RNA by nuclease digestion (13, 28). In addition to full-length and internally processed forms, both the VPg domain and full-length NIa have been detected in polyprotein forms with the 6-kDa protein, which is positioned adjacent to the N terminus of NIa within the viral polyprotein (35). The 6-kDa protein possesses membrane-binding activity and is required for genome amplification (35).

Although TEV RNA replication likely occurs in association with cytoplasmic membranes (25), NIa and the RNA polymerase, NIb, accumulate primarily in the nuclei of infected cells (3, 4, 33). Both NIa and NIb contain independent nuclear localization signals (NLSs) (23, 33). The NIa NLS is located within the amino terminal 72 residues of the VPg domain (11). The role of these proteins in the nucleus is not known. It was postulated that a proportion of NIa is directed to membranous replication sites in a polyprotein form containing the 6-kDa protein (34, 35). The membrane-binding activity of the 6-kDa protein was shown to override the nuclear localization activity of NIa when both were present within a polyprotein (34).

In this study, a functional analysis of four NIa activities was conducted. The NLS was mapped more precisely using transgenic plants expressing NIa-containing fusion proteins. Modified TEV genomes encoding NIa molecules with altered nuclear localization activity, VPg activity, internal cleavage activity, and *trans*-proteolytic activity were generated, and effects on genome amplification were investigated. Additionally, the ability of wild-type NIa protein supplied in *trans* to complement the NIa mutant viruses was tested.

* Corresponding author. Fax: (409) 845-2891. Electronic mail address: carrington@bio.tamu.edu.

MATERIALS AND METHODS

Plant lines and antisera. *Nicotiana tabacum* cv. Xanthi nc was used for isolation of protoplasts, whole-plant inoculation, and preparation of transgenic plants. Anti-NIa, anti-NIb, and anti-cylindrical inclusion (CI) polyclonal antibodies and anti-NIa monoclonal antibodies were described previously (33, 39).

Transgenic plants expressing NIa-containing proteins. Plasmid pRTL2 was used as a base vector for most constructs. This plasmid contains the cauliflower mosaic virus 35S promoter with duplicated enhancer sequence, the TEV 5′ nontranslated region, a polylinker sequence, and the cauliflower mosaic virus 35S polyadenylation signal. pRTL2-GUS and pRTL2-GUS/NIa, which contain the coding sequences for β-glucuronidase (GUS) and the GUS/NIa fusion protein, respectively, were described previously (33). A series of plasmids containing the NIa sequence coding for amino acid residues 43 to 46, 40 to 46, 43 to 49, or 40 to 49 fused to the 3′ end of the GUS sequence was constructed. pRTL2S-G/43-46 was generated by ligation of a double-stranded synthetic oligonucleotide (with *Bgl*II and *Bam*HI sites at the 5′ and 3′ termini, respectively) between the *Bgl*II and *Bam*HI sites of pL.GUS/NIb (23). This resulted in replacement of the NIb coding sequence with codons 43 to 46 from NIa. pRTL2S-G/40-46 and pRTL2S-G/43-49 were constructed by site-directed insertional mutagenesis of pRTL2S-G/43-46 by using oligonucleotides representing NIa codons 40 to 42 and 47 to 49, respectively. pRTL2S-G/40-49 was constructed by site-directed insertional mutagenesis of pRTL2S-G/43-49 by using an oligonucleotide corresponding to NIa codons 40 to 42.

A series of pRTL2-GUS/NIa-derived plasmids containing single-codon substitutions in the NIa sequence between positions 40 and 48 was generated. Site-directed mutagenesis of pRTL2-GUS/NIa was carried out to change each of the positions between 40 and 48 to either an Ala or a Ser codon. Each mutant was named according to the single-letter code for the amino acid residue in the wild-type sequence, the position occupied by that residue in NIa, and the mutant residue. For example, a mutant encoding a fusion protein in which Asn at position 40 was changed to Ala was named N40A.

The expression cassettes were excised from the pRTL2-based plasmids by *Hin*dIII digestion and subcloned into the binary vector, pGA482 (2). These plasmids were mobilized into *Agrobacterium tumefaciens*. Transgenic tobacco plants were generated by *A. tumefaciens*-mediated gene transfer using kanamycin selection as described previously (12).

Transgenic plants expressing the NIa, 6-kDa protein/NIa (6/NIa), and CI/6/NIa regions of the TEV genome were also produced. The NIa and 6/NIa coding sequences were amplified by PCR, using as the template plasmid pTL7SN-6/NIa/NIb. The CI/6/NIa coding sequence was amplified from plasmid pTEV7DA, which contains a full-length cDNA representing the viral genome (14). The 5′ PCR primers included an *Nco*I site and resulted in addition of two non-TEV-derived codons. The 3′ primers included a stop codon and a *Kpn*I site. Amplification products were inserted between the *Nco*I and *Kpn*I sites of the intermediate plasmid, pTL7SN (12), which contains an SP6 bacteriophage transcriptional promoter for in vitro transcription. The integrity of the coding sequences in these three plasmids was verified by in vitro transcription followed by cell-free translation of the transcripts in a rabbit reticulocyte lysate system. The cDNA fragments were then subcloned from the pTL7SN-derived plasmids into a modified binary plasmid, pGAdek.G/NIb.L, containing the cauliflower mosaic virus 35S promoter and terminator. These plasmids were transferred to *A. tumefaciens* and used for plant transformation.

Expression of the transgene products was tested in the R1 generation. For plants expressing NIa, 6/NIa, and CI/6/NIa, total sodium dodecyl sulfate (SDS)-soluble protein was extracted from kanamycin-resistant plants and subjected to immunoblot analysis using polyclonal anti-NIa serum and a chemiluminescence detection system (Amersham). For plants expressing GUS fusion proteins, the transgenic proteins were detected by immunoblot analysis with anti-GUS polyclonal serum and by GUS activity assay using the fluorometric substrate 4-methylumbelliferyl-β-D-glucuronide (22). Nuclear localization of the GUS/NIa fusion proteins was assayed in situ (33). Epidermal strips were peeled from the abaxial surface of leaves and incubated with the colorimetric substrate 5-bromo-4-chloro-3-indolyl-β-D-glucuronic acid (X-Gluc). GUS activity in nuclear or nonnuclear compartments was visualized by the formation of a blue precipitate.

NIa mutations within the TEV-GUS genome. Mutations affecting NIa positions 40 to 48 were introduced by oligonucleotide-directed mutagenesis into pTL7SN-5471, which contains DNA representing TEV genome nucleotides 5412 to 7098. Single codon mutations were identical to those described above. Double and triple codon mutations affecting positions 41, 43, and 44 were also introduced. Codons for Lys-41, Lys-43, and Arg-44 were changed to codons for Ala in all dual (41-43, 41-44, and 43-44 mutations) and triple (41-43-44 mutation) combinations. These mutations were introduced into plasmid pTEV7DAN-GUS (14) by transfer of the *Eco*NI-*Bam*HI fragment representing genome nucleotides 5468 to 5916. pTEV7DAN-GUS contains a full-length cDNA representing the TEV genome with the coding sequence for GUS inserted between the P1 and HC-Pro coding regions (Fig. 1). An SP6 promoter adjacent to the 5′ end of the TEV sequence permits synthesis of transcripts in vitro.

Mutations converting codons for Tyr-62 (Y62A mutation) or Cys-339 (C339A mutation) of NIa to Ala codons were generated by oligonucleotide-directed mutagenesis of pTL7SN-5471 or pTL7SN-6/NIa/NIb, respectively. The mutations were introduced into pTEV7DAN-GUS by transfer of the *Eco*NI-*Bam*HI fragment containing nucleotides 5468 to 5916 (Y62A) or the *Bam*HI-*Sal*I fragment containing nucleotides 5916 to 7171 (C339A).

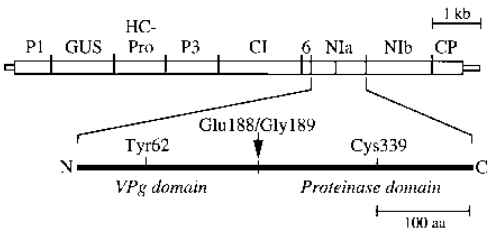

FIG. 1. Diagrammatic representation of the TEV genome and NIa. The genome map of coding (thick box) and noncoding (thin boxes) sequences is drawn to scale at the top. The individual coding regions are indicated above the diagram. An enlarged diagram of NIa is drawn at the bottom. The arrow between Glu-188 and Gly-189 indicates the site of internal cleavage between the N-terminal VPg domain and the C-terminal proteinase domain. The positions of residues critical for RNA attachment (Tyr-62) and proteinase activity (Cys-339) are indicated. aa, amino acids.

Three mutations affecting codons for the P1 (Thr-186) and P3 (Glu-188) positions of the NIa internal cleavage site were introduced into pTL7SN.5472. This plasmid contains cDNA representing TEV nucleotides 5412 to 7171. The codons for Thr-186 and Glu-188 were changed to codons for Tyr and Gln in the T186Y and E188Q mutants, respectively. A double mutation termed T186Y/E188Q was also generated. These mutations were introduced into pTEV7DAN-GUS by transfer of the *Bam*HI-*Sal*I fragment representing TEV nucleotides 5916 to 7171.

In vitro transcription and translation. In vitro transcription with SP6 polymerase was used to produce RNA transcripts for in vitro translation. Transcripts were synthesized by using *Pvu*II-linearized pTL7SN-derived plasmids. Transcripts were recovered from the reactions by precipitation in the presence of 70% ethanol. Translation reactions were done with rabbit reticulocyte lysate (Promega). For pulse-chase experiments, ^{35}S-labeled products in 100-μl reactions were generated for 10 min in the presence of 88 μCi of [^{35}S]methionine (DuPont-NEN), after which nonlabeled methionine was added to a concentration of 50 mM. Aliquots (10 μl) were removed at 0, 5, 10, 20, 40, and 80 min after initiation of the chase period and added to 20 μl of protein dissociation buffer. Phenylmethylsulfonyl fluoride was added to the chase mixture to a final concentration of 1 mM at the 10-min time point. The samples were analyzed by SDS–12.5% polyacrylamide gel electrophoresis and autoradiography.

Inoculation of protoplasts and plants with in vitro-synthesized transcripts. In vitro synthesis of m^{7}GpppG-capped transcripts from pTEV7DAN-GUS by using SP6 polymerase (Ambion) was described previously (14). Approximately 10 μg of transcripts was introduced into protoplasts by the polyethylene glycol-mediated transfection method (30). Protoplasts were harvested at 24, 48, and 72 h postinoculation (p.i.), and GUS activity was measured by the fluorometric assay. Activity values were calculated as picomoles of substrate cleaved per minute per 10^5 protoplasts. In all experiments, protoplasts were also inoculated in parallel with transcripts representing parental TEV-GUS and TEV-GUS/VNN mutant genomes. The TEV-GUS/VNN mutant contained a replication-debilitating mutation affecting a conserved motif within NIb polymerase (24). Approximately 2-μg aliquots of transcripts were used to inoculate each of two carborundum-dusted leaves of plants. Infection was scored as positive by the appearance of symptoms and/or by detection of GUS activity in leaves two nodes above the inoculated leaves.

Immunofluorescence microscopy. Protoplasts were isolated from systemically infected leaves of plants at 6 days p.i. Leaves were infiltrated with a solution containing cell wall-degrading enzymes and incubated for 2 to 3 h at room temperature. The released protoplasts were isolated as described previously (10). The protoplasts (approximately 5×10^5) were fixed in 1 ml of FAA (4% paraformaldehyde, 5% acetic acid, 50% ethanol) in a 1.5-ml Eppendorf tube for 1 h at room temperature. After sedimentation at $80 \times g$ in an M4 swinging-bucket rotor in a Jouan CR412 centrifuge, the samples were incubated in two changes of 95% ethanol for 30 min. The protoplasts were rehydrated through a series of ethanol–1× phosphate-buffered (PBS; 140 mM NaCl, 2.5 mM KCl, 10 mM Na_2HPO_4, 1.5 mM KH_2PO_4) washes starting with 75% ethanol, followed by 50, 25, and 0% steps.

The samples were rotated for 1 h at 4°C in blocking solution (1× PBS, 5% dry milk, 5% goat serum, 5% sheep serum). The first antibodies (polyclonal NIb and monoclonal NIa) were added to samples simultaneously each at a 1:100 dilution (10 μl in 1 ml) in blocking buffer and rotated for 1 h at room temperature. The monoclonal NIa antibody contained a mix of 12 monoclonal antibodies from mouse acites fluid and was described previously (39). The protoplasts were washed five times (5 to 10 min for each wash) in 1× PBS-Tween (1× PBS, 0.1% bovine serum albumin, 0.05% sodium azide [pH 7.2], 0.05% Tween 20). The second antibody was a mixture of fluorescein isothiocyanate (FITC)-conjugated goat anti-mouse immunoglobulin G (IgG; Sigma) at 1:100 dilution and Cy3-

conjugated sheep anti-rabbit IgG at 1:200 dilution in blocking buffer. Cells were rotated for 1 h at room temperature. The samples were then washed five times in 1× PBS-Tween (5 to 10 min for each wash). With the second wash, 4′,6-diamidino-2-phenylindole (DAPI; 0.5 mg/ml; Sigma) was added, and the mixture was incubated for 30 min at room temperature.

After the last centrifugation step, as much liquid as possible was removed from the samples. One drop of equilibration buffer (component C; Molecular Probes, Inc., Eugene, Oreg.) was added to the protoplast pellet, and the mixture was incubated at room temperature for 10 min. Two drops of SlowFade-Light in 50% glycerol (Molecular Probes) was added, and the sample (25 μl) was mounted on a glass slide with a coverslip. Immunofluorescence microscopy was conducted with an Olympus BX50 microscope equipped with several filter sets. For detection of DAPI fluorescence, the DM400 dichroic mirror/BP360-370 exciter filter/BA420 barrier filter set was used. For detection of FITC fluorescence, the DM500 dichroic mirror/BP470-490 exciter filter/BA515 barrier filter set was used. For detection of Cy3 fluorescence, the DM570 dichroic mirror/BP530-550 exciter filter/BA590 barrier filter set was used. Photomicrographs were taken with Kodak Ektachrome 400 film. Nuclear localization activity of NIa encoded by various mutants was assessed by scoring between 100 and 152 protoplasts. The percentage of cells containing NIa that was predominantly nuclear, partially nuclear/partially cytoplasmic, or predominantly cytoplasmic was recorded.

RESULTS

This study was undertaken to further understand the multiple roles of the NIa protein in infected cells. First, the effects of mutations altering the NLS and VPg-RNA attachment site on subcellular transport of NIa and viral genome amplification were tested. Second, the effects of substitutions affecting the NIa internal cleavage site and proteinase active site on proteolytic activity and genome amplification were investigated. Third, the ability of mutant genomes encoding defective NIa molecules to be complemented by NIa supplied in *trans* was investigated by using a transgenic approach.

Mapping the NIa NLS. From results of assays using transient and transgenic assays with GUS/NIa fusion proteins, two regions within NIa were proposed previously to contribute to nuclear translocation activity (11). A region between residues 43 and 72 was sufficient for nuclear transport of a GUS fusion protein in transgenic cells, although transport was stimulated by the presence of an N-terminal sequence. In protoplast transient assays, efficient transport required residues 1 to 72. The sequence between residues 41 and 49 contains five basic (Arg or Lys) residues and possesses a general similarity to the simian virus 40 large-T-antigen-type NLS (32). To test the hypothesis that this sequence contains an autonomous NLS, GUS fusion proteins containing all or part of NIa residues 40 to 49 were expressed in transgenic plants and their subcellular localization properties were analyzed (Fig. 2). As controls, transgenic plants expressing nonfused GUS and GUS/NIa were analyzed in parallel. Nonfused GUS was confined to the cytoplasm, whereas GUS/NIa accumulated in the nucleus (Fig. 3A). As observed previously (11, 33), the X-Gluc product was concentrated within the nucleolar region of GUS/NIa-transformed cells. In situ localization revealed that GUS/40-49 accumulated primarily in the nucleus (Fig. 2 and 3A). GUS activity from transgenic cells expressing GUS/40-46 and GUS/43-46 was located in the cytoplasm, while activity in plants expressing GUS/43-49 was located in both the cytoplasm and the nucleus (Fig. 2). These results indicate that an autonomous signal for nuclear localization of GUS fusion proteins resides within NIa residues 40 to 49.

The role of residues at NIa positions 40 to 48 in translocation of GUS/NIa fusion protein in transgenic cells was tested. Mutations resulting in substitution of Ala or Ser in place of each residue were introduced, and subcellular localization in epidermal cells was analyzed. The fusion proteins containing the N40A, K45A, and T47A substitutions were localized predominantly to the nucleus (Fig. 2). The fusion proteins containing G42S and G46S substitutions partitioned between the nucleus and cytoplasm. Fusion proteins with the K41A, K43A, R44A, and T48A substitutions were localized exclusively to the cytoplasm. These results suggest that K41, K43, R44, and T47 are necessary for efficient nuclear transport of the GUS/NIa fusion proteins in transgenic cells.

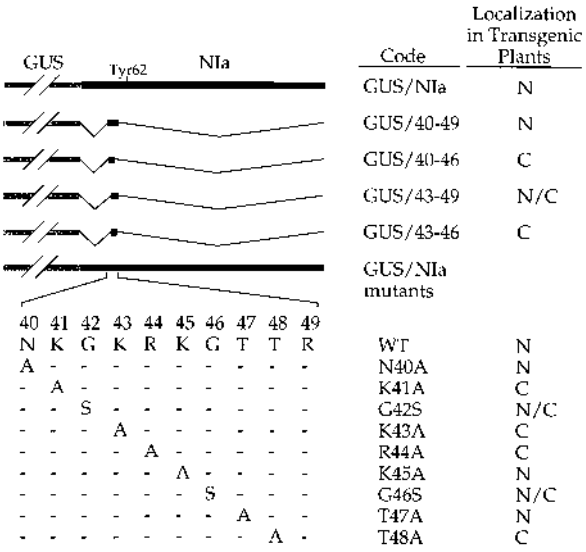

FIG. 2. Diagrammatic representation of GUS/NIa fusion proteins. The coding sequences for GUS and part or all of NIa were fused and expressed in transgenic plants. The amino acid sequence (single-letter code) between NIa positions 40 and 49, as well as the substitutions introduced in this region, are enlarged at the bottom. The nuclear localization phenotype of each fusion protein is indicated on the right. Abbreviations: C, cytoplasmic; N, nuclear; N/C, partially nuclear/partially cytoplasmic.

Effects of VPg domain mutations on genome amplification. The VPg domain has two identifiable activities: it attaches covalently to viral RNA at Tyr-62, and it contains an NLS between positions 40 and 49. Mutations affecting each of these activities were introduced into the TEV-GUS genome. The TEV-GUS genome encodes GUS as a reporter and has proven useful for quantitative analyses of numerous TEV mutants. The Tyr-62 codon of NIa was changed to an Ala codon in the TEV-GUS/Y62A mutant. Single codon mutations affecting seven positions within the NLS sequence were also introduced into the TEV-GUS genome. Capped transcripts were synthesized and used to inoculate protoplasts and plants. In the protoplast experiments, samples were analyzed for GUS activity at 24, 48, and 72 h p.i. Inoculations with each mutant were repeated at least four times. As controls, cells were also inoculated in parallel with transcripts representing parental TEV-GUS and the replication-defective TEV-GUS/VNN mutant (24). For whole-plant experiments, systemic infection was scored by the appearance of symptoms and/or by detection of GUS activity in noninoculated leaves.

The TEV-GUS/Y62A mutant failed to induce levels of GUS activity in protoplasts above that of the amplification-defective control and failed to infect plants systemically (Table 1). This result indicated, not surprisingly, that the VPg attachment site is critical for virus infectivity. In contrast, all of the genomes harboring single codon changes affecting the NLS were amplified with relative efficiencies ranging between 13 and 209% of the parental TEV-GUS level (Table 1). The most debilitated mutant (K45A) contained a substitution that had no effect on nuclear localization of the GUS/NIa fusion protein in transgenic plants. The mutants containing substitutions affecting residues required for NLS activity in transgenic plants (K41A,

K43A, R44A, and T48A) were amplified to at least 35% the level of parental virus. Each mutant was also able to infect plants systemically (Table 1).

The finding that mutations affecting positions required for nuclear transport of GUS/NIa had relatively little effect on genome amplification could be explained in one of two ways. The nuclear transport activity of NIa might have little or no effect on genome amplification. Alternatively, nuclear transport of the mutant NIa proteins in infected cells might be less affected by the K41A, K43A, and R44A mutations than was the GUS/NIa fusion protein in transgenic cells. To determine if the NIa proteins encoded by the K41A, K43A, and R44A mutants were localized to the nucleus in infected cells, immunofluorescence analysis using NIa monoclonal antibodies was performed with protoplasts isolated from infected leaf tissue. The distribution of NIa in at least 100 infected cells was determined. The NIa pool encoded by the parental TEV-GUS genome was located exclusively or predominantly in the nucleus in 90.1% of the cells and was divided between the nuclear and cytoplasmic compartments in the remaining 9.9% of cells (Fig. 3B and Table 1). Similarly, NIa encoded by the K41A, K43A, and R44A mutants was predominately nuclear (68 to 89%), with some cells displaying partial cytoplasmic/partial nuclear localization (11 to 32%). In no case was the NIa localization phenotype exclusively cytoplasmic (Table 1). It was concluded, therefore, that the single codon mutations that debilitated GUS/NIa transport were insufficient to effectively debilitate NIa transport in virus-infected cells.

Additional mutant TEV-GUS genomes were produced in which the K41A, K43A, and R44A mutations were introduced in double (41-43, 41-44, and 43-44 mutants) and triple (41-43-44) combinations. Genome amplification in protoplasts, infectivity in plants and NIa nuclear localization properties were assayed. The double mutants were amplified to levels considerably lower than those for any of the single-codon K41A, K43A, and R44A mutants (2.3 to 15.7% relative to parental TEV-GUS). The proportion of plants that became systemically infected after inoculation was lower with the double mutants (Table 1), although the timing of symptom development in noninoculated leaves was similar to that for the parental virus (data not shown). The 41-43-44 NLS triple mutant was amplified to a level approximately 500-fold lower than that of the parental virus and failed to infect any inoculated plants (Table 1).

Protoplasts from symptomatic tissue of plants infected by the double-mutant viruses were subjected to immunofluorescence analysis. As an internal nuclear localization control, cells were colabeled with rabbit anti-NIb and mouse monoclonal anti-NIa sera. An FITC-labeled second antibody was used to visualize NIa, and a Cy3-labeled second antibody was used to detect NIb. A minor problem encountered with use of the red-fluorescing Cy3 was autofluorescence from chloroplasts. Although this problem was minimized by several ethanol extraction steps after protoplast fixation, the ability to detect low levels of NIb in the cytoplasm was marginal. Cells were also treated with DAPI to detect the positions of nuclei within cells. Each fluorescence marker was visualized by using a distinct UV filter set. Because of the lower levels of amplification, the intensity of the NIa and NIb signals in mutant-infected cells was lower than in parental virus-infected cells. In contrast to the NLS single mutants, the double mutants encoded NIa proteins with clear defects in nuclear localization (Fig. 3B and Table 1). The 41-43 and 43-44 mutants exhibited NIa localization phenotypes in which at least 81% of cells showed partial nuclear/partial cytoplasmic NIa or predominantly cytoplasmic NIa. The NIa encoded by the 41-44 mutant was predominantly

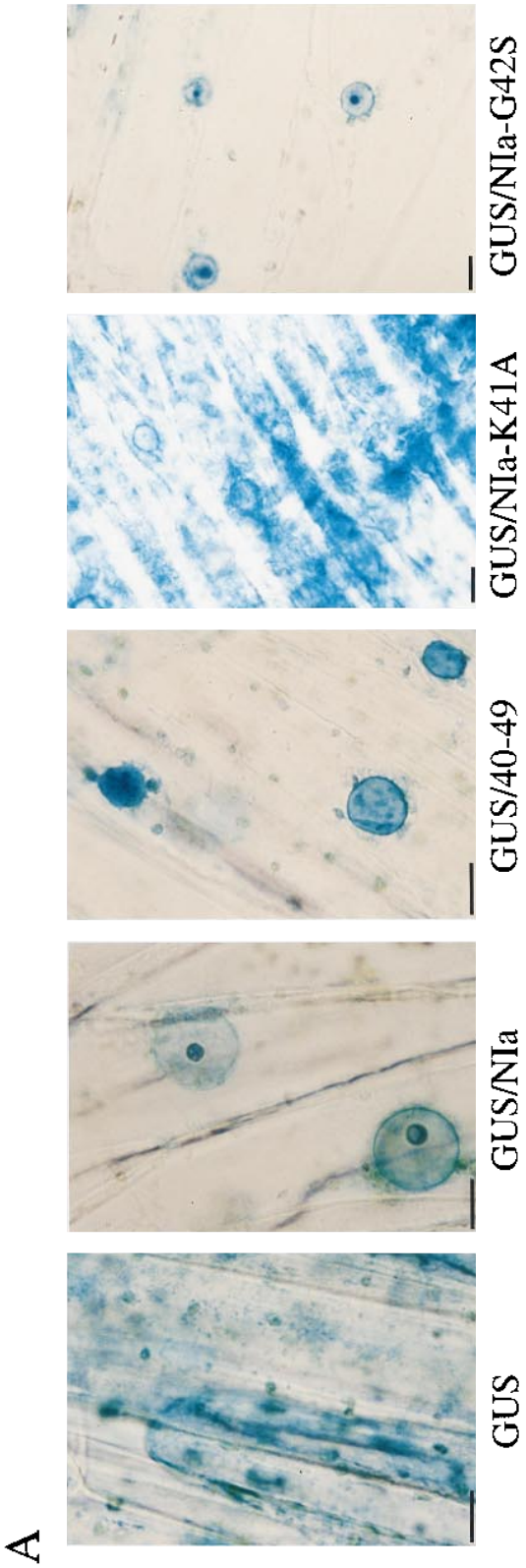

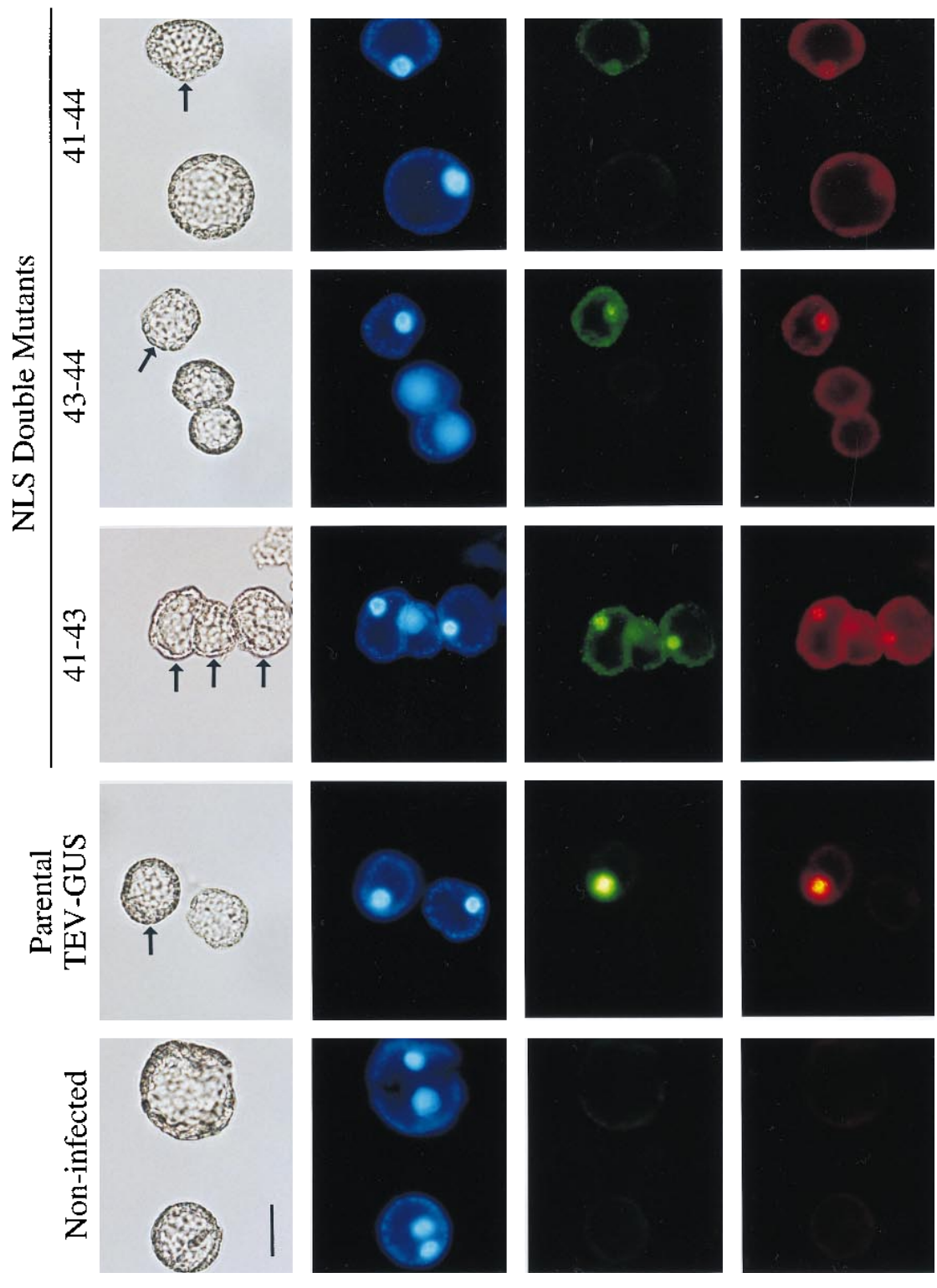

FIG. 3. Effects of NLS mutations on NIa-mediated nuclear translocation in transgenic and infected cells. (A) In situ localization of GUS activity in epidermal cells of transgenic plants expressing selected GUS/NIa fusion proteins. Epidermal strips from transgenic plants were incubated with the colorometric substrate (X-Gluc), which forms a blue reaction product in the presence of GUS. Bars equal 20 μm. (B) Immunofluorescence localization of NIa and NIb in protoplasts infected by parental TEV-GUS or the NLS double mutants. Protoplasts were prepared from systemically infected leaves at 6 days p.i., fixed, and incubated simultaneously with anti-NIa mouse monoclonal antibody and anti-NIb rabbit polyclonal antibody. The protoplasts were then incubated simultaneously with FITC-linked anti-mouse IgG and Cy3-linked anti-rabbit IgG second antibodies. The cells were washed, incubated with DAPI, and mounted in SlowFade-Light. Four photomicrographs using various filter combinations were taken for each field of view to show a bright-field image, DAPI fluorescence (nuclei), FITC fluorescence (anti-NIa [α-NIa]), or Cy3 fluorescence (anti-NIb [α-NIb]), as indicated at the left. Arrows in the bright-field images indicate the infected cells; cells without arrows were not infected. The bar equal 35 μm.

TABLE 1. Amplification and NIa nuclear localization phenotypes of TEV-GUS containing mutations in the NLS and VPg active site

Mutant code	Relative amplification[a] ± SD	Systemic infection in plants[b] (no. infected/no. tested)	NIa nuclear localization phenotype[c]		
			Nuclear only	Nuclear/cytoplasmic	Cytoplasmic only
TEV-GUS	100	19/24	90.1	9.9	0.0
N40A	209.5 ± 20.0	8/8	—	—	—
K41A	35.8 ± 13.3	8/8	68	32	0
K43A	68.9 ± 7.3	8/10	76	24	0
R44A	85.1 ± 9.0	8/10	89	11	0
K45A	13.5 ± 0.5	5/10	—	—	—
T47A	76.8 ± 16.3	8/8	—	—	—
T48A	118.0 ± 43.0	8/8	—	—	—
41-43	9.4 ± 4.9	1/10	12	48	40
41-44	2.3 ± 2.0	1/10	0	17	83
43-44	15.7 ± 7.6	4/10	19	62	19
41-43-44	0.2 ± 0.1	0/13	—	—	—
Y62A	0.04 ± 0.02	0/10	—	—	—

[a] Relative amplification at 48 h p.i. of each mutant was determined as follows: (GUS activity in sample virus-infected cells/GUS activity in parental TEV-GUS-infected cells) × 100.
[b] Determined by the appearance of symptoms and/or detection of GUS activity in upper, noninoculated leaves.
[c] The subcellular distribution of NIa in at least 100 protoplasts was determined by immunofluorescence microscopy. The percentages of cells in which NIa was detected exclusively in the nucleus (nuclear only), partially in the nucleus and partially in the cytoplasm (nuclear/cytoplasmic), and exclusively in the cytoplasm (cytoplasmic only) are shown. —, not tested.

cytoplasmic. The NIb pools in cells infected by each double mutant were predominantly nuclear (Fig. 3B), although in the case of the 41-44 mutant, the low level of accumulation would have rendered fluorescence in the cytoplasm difficult to detect. These experiments reveal that the effects of the K41A, K43A, and R44A mutations on genome amplification and NIa nuclear localization are synergistic. They also show a correlation between the extent of debilitation of genome amplification and the degree of inhibition of NIa nuclear localization.

Effects of NIa proteinase and internal cleavage site mutations. The NIa proteinase catalyzes cleavage of the TEV polyprotein at six positions. Mutations that inactivate cleavage site function at several of these positions, including the internal NIa cleavage site, debilitate genome amplification (13, 35). The proteinase-inactivating C339A mutation, which results in substitution of Ala for the active-site Cys-339 residue, was introduced into the TEV-GUS genome. Transcripts representing the TEV-GUS/C339A genome were unable to amplify in protoplasts (Table 2).

The NIa internal cleavage site is processed incompletely in infected cells and inefficiently after synthesis in vitro (13, 16). The slow internal cleavage site activity may be due to an inefficient heptapeptide motif surrounding the scissile bond between Glu-188 and Gly-189. The internal cleavage site heptapeptide, Glu-Asp-Leu-Thr-Phe-Glu ↓ Gly, differs from the consensus NIa recognition motif, Glu-Xaa-Xaa-Tyr-Xaa-Gln ↓ Gly or Ser, at the P1 and P3 positions. The P1, P3, and P6 positions were demonstrated to be crucial for efficient cleavage site utilization (15). To test the hypothesis that Glu at position P1 and Thr at position P3 contribute to inefficient internal cleavage site activity, single (T186Y and E188Q) and double (T186Y/E188Q) substitutions of Tyr and Gln for Thr-186 (P1) and Glu-188 (P3), respectively, were introduced into plasmid pTL7SN-5472. Transcripts derived from this plasmid encode a 68-kDa polyprotein consisting of the C-terminal region of CI, 6-kDa protein, NIa, and the N-terminal part of NIb (Fig. 4A). This polyprotein contains four NIa cleavage sites, including the internal site. Each mutant polyprotein, therefore, contained functional cleavage sites that served as controls for NIa proteolytic activity. In pulse-chase experiments using the polyprotein synthesized in vitro from the wild-type plasmid, processing at the sites to yield 49-kDa NIa was detected within 5 min after initiation of the chase and continued to near completion within 80 min (Fig. 4B). The NIa protein migrated as a doublet during electrophoresis, with the larger band increasing in intensity over the time course. The NIa protein was relatively stable for the duration of the chase, indicating that processing at the internal cleavage site was extremely inefficient. A polyprotein containing the C339A active-site substitution failed to undergo proteolysis during the 80-min chase (Fig. 4C).

The processing patterns of three polyproteins containing the internal cleavage site substitutions differed from the wild-type pattern. In each case, four smaller processing products (labeled 1, 2, 3, and 4) were detected, and NIa was less stable over the 80-min chase period (Fig. 4B and C). The smaller products derived from the E188Q mutant polyprotein were detected by 10 to 20 min, while the smaller products from the T186Y and the T186Y/E188Q mutant polyproteins were detected within 5 to 10 min. The T186Y/E188Q polyprotein processed most efficiently over the time course, and a precursor-product relationship between NIa-containing proteins and the smaller products was clearly observed. To determine the nature of the smaller products, immunoprecipitation analysis with poly-

TABLE 2. Relative amplification of TEV-GUS NIa mutants in transgenic cells

Mutant code	Relative amplification in protoplasts[a] ± SD			
	Nontransgenic Xanthi nc	Transgenic protoplasts		
		NIa	6/NIa	CI/6/NIa
TEV-GUS	100	100	100	100
VNN	0.01 ± 0.01	0.01 ± 0.00	0.01 ± 0.00	0.01 ± 0.00
C339A	0.02 ± 0.01	0.01 ± 0.00	0.01 ± 0.00	0.02 ± 0.01
Y62A	0.04 ± 0.02	0.11 ± 0.01	0.00 ± 0.00	0.03 ± 0.02
T186Y	0.01 ± 0.01	0.01 ± 0.00	0.01 ± 0.00	0.06 ± 0.03
E188Q	3.5 ± 0.2	0.22 ± 0.15	2.7 ± 0.4	0.69 ± 0.17
T186Y/E188Q	0.01 ± 0.00	0.01 ± 0.00	0.01 ± 0.00	0.02 ± 0.00
41-43	13.6 ± 1.6	7.9 ± 0.2	23.8 ± 3.9	14.6 ± 7.5
41-44	4.7 ± 0.8	0.36 ± 0.11	1.9 ± 0.16	0.84 ± 0.08
43-44	20.9 ± 2.9	12.8 ± 0.5	27.8 ± 0.4	15.0 ± 4.1
41-43-44	0.29 ± 0.04	0.07 ± 0.01	0.14 ± 0.04	0.31 ± 0.15

[a] See Table 1, footnote *a*, for calculation of relative amplification levels.

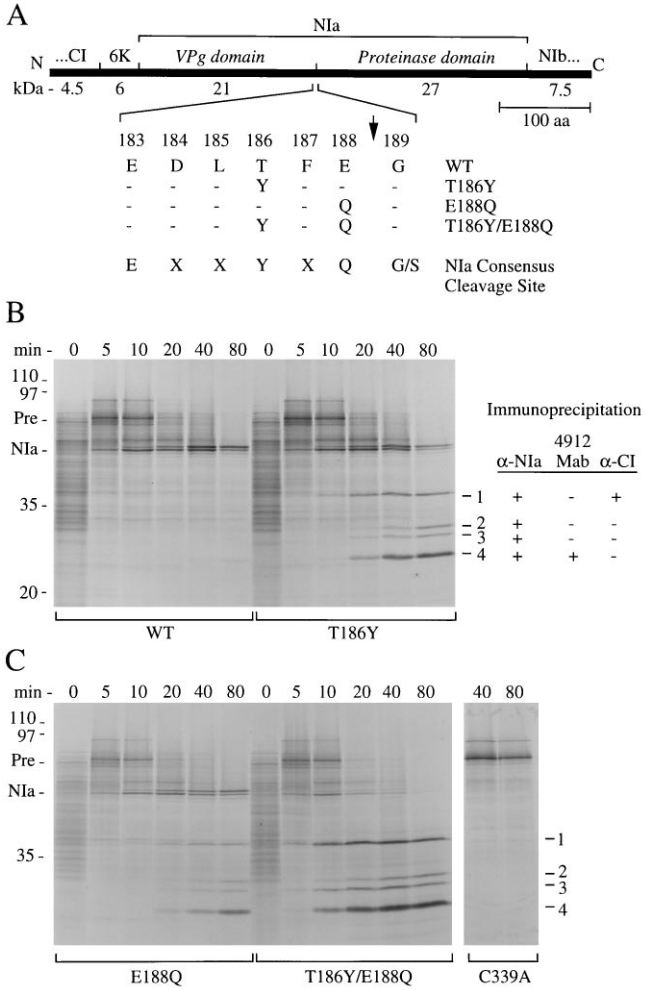

FIG. 4. Effects of internal cleavage site modifications on NIa internal processing. (A) Diagrammatic representation of the polyprotein encoded by plasmid pTL7SN-5472. The wild-type and mutant sequences of the internal cleavage site are indicated in the enlarged segment. aa, amino acids. (B and C) Pulse-chase analysis of polyproteins containing a wild-type (WT) or mutant (T186Y, E188Q, and T186Y/E188Q) internal cleavage site. Radiolabeling with [^{35}S]methionine for 10 min was followed by addition of excess nonlabeled methionine. Samples were withdrawn at the chase times indicated above the lanes. The C339A polyprotein (C) served as a proteinase-defective control. The electrophoretic positions of polyprotein precursors (Pre), NIa protein, and molecular weight markers (in kilodaltons) are shown on the left. The positions of the four products resulting from internal NIa cleavage are shown on the right (1 to 4). The immunoprecipitation profiles of the internal cleavage products obtained by using polyclonal anti-NIa (α-NIa), monoclonal anti-proteinase domain (4912 Mab), and polyclonal anti-CI (α-CI) sera are shown at the right in panel B.

clonal anti-CI, polyclonal anti-NIa, and monoclonal anti-proteinase domain sera was conducted by using the total processing products from the T186Y polyprotein (Fig. 4B). Each of the smaller products was immunoprecipitated with polyclonal anti-NIa serum, indicating that each contained part of NIa. The anti-CI serum precipitated exclusively polypeptide 1, which migrated in SDS-polyacrylamide gels with an apparent molecular mass of 34 kDa. The anti-proteinase domain serum precipitated exclusively polypeptide 4, which migrated with an apparent molecular mass of 25 kDa. The immunoprecipitation profiles suggested that polypeptide 1 contained the CI-6-VPg domain region of the polyprotein and that polypeptide 4 contained only the proteinase domain. Polypeptides 2 and 3 were precipitated with neither the anti-CI nor the anti-proteinase domain serum, and their identities were not investigated further. However, at least one of these likely corresponds to the 6/VPg polypeptide. These results suggested that changing the cleavage site from a suboptimal to an optimal context markedly enhanced internal processing of NIa.

To determine the effects of accelerated internal NIa cleavage on TEV-GUS genome amplification, mutant genomes containing the T186Y, E188Q, and T186Y/E188Q modifications were generated and introduced into protoplasts. Each of the mutants was debilitated compared with parental TEV-GUS (Fig. 5 and Table 2). The E188Q mutant amplified to 3.5% the level of the parental virus (48 h p.i.). The T186Y and T186Y/E188Q mutants failed to amplify and were indistinguishable from the replication-defective VNN mutant. These results suggest that the suboptimal context of the internal cleavage site is required for efficient genome amplification.

Transgenic complementation analysis. A transgenic complementation approach has been used to demonstrate that at least two TEV-encoded proteins provide *trans*-active functions to promote genome amplification. Mutants with defects in the NIb polymerase, such as the VNN mutant, or mutants that lack the NIb sequence altogether can be complemented by wild-type, mature NIb supplied by transgenic cells (24). Amplification of deletion mutants lacking the P1 coding region can be stimulated by infection of P1-expressing transgenic cells (41). To determine if any of the defective genomes analyzed here could be rescued by NIa in *trans*, a similar transgenic complementation strategy was used. Transgenic plants expressing NIa were produced. Because of the possibility that some NIa functions require a polyprotein context, transgenic plants expressing 6/NIa and CI/6/NIa were also produced (Fig. 6A). These polyproteins were predicted to undergo NIa-mediated proteolysis within the transgenic cells. Immunoblot analysis of protein extracts from transgenic plants indicated that each line accumulated mature, processed NIa (Fig. 6B). No NIa-containing polyproteins were detected in 6/NIa or CI/6/NIa plants, indicating that the proteolytic activity of NIa was functional. Expression of the 6/NIa or CI/6/NIa transgene was further confirmed by RNA blot analysis using radiolabeled probes specific for either the CI or 6-kDa protein coding sequence (data not shown). Complementation experiments were conducted with one NIa, one 6/NIa, and three CI/6/NIa transgenic lines. Protoplasts from nontransgenic and transgenic plants were inoculated with mutant transcripts encoding NIa variants with defects in the VPg attachment site (Y62A), proteinase

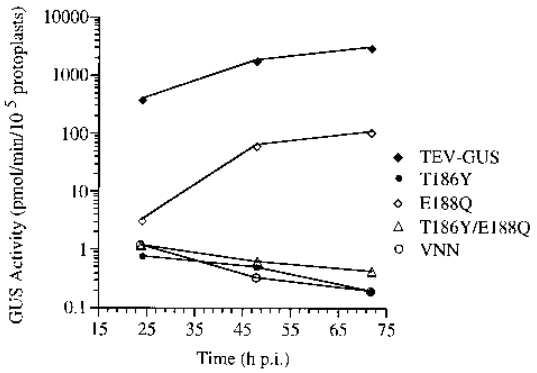

FIG. 5. Effect of the NIa internal cleavage site mutations on TEV-GUS amplification in protoplasts. GUS activity (picomoles of substrate cleaved per minute per 10^5 protoplasts) was measured in protoplasts inoculated with parental TEV-GUS or the VNN, T186Y, E188Q, or T186Y/E188Q mutant at 24, 48, and 72 h p.i.

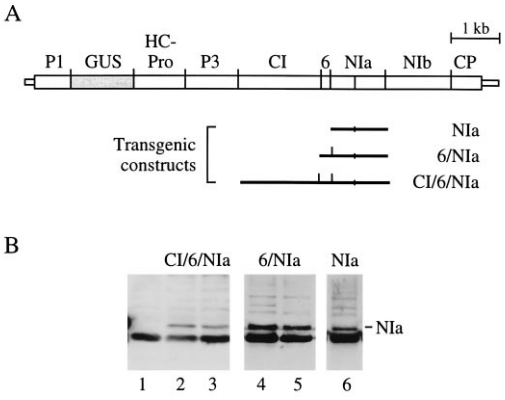

FIG. 6. Transgenic plants expressing NIa. (A) Diagrammatic representation of TEV genome regions expressed in transgenic plants. (B) Immunoblot analysis of extracts from nontransgenic and transgenic plants, using polyclonal anti-NIa serum. Immunoreactive proteins were detected by using a chemiluminescent second-antibody system. The electrophoretic position of NIa is indicated. Lane 1, nontransgenic plant; lanes 2 and 3, two independent CI/6/NIa transgenic plants; lanes 4 and 5, two independent 6/NIa transgenic plants; lane 6, NIa transgenic plant.

active site (C339A), internal cleavage site (T186Y, E188Q, and T186Y/E188Q), and NLS sequence (41-43, 41-44, 43-44, and 41-43-44). Parental TEV-GUS and VNN mutant transcripts were also tested in parallel in all experiments.

Genome amplification data for transgenic complementation experiments are presented in Table 2. Parental TEV-GUS was amplified to equivalent levels in protoplasts from each plant line. No consistent pattern of stimulation of genome amplification was detected with any of the NIa mutant viruses. Those mutants with severe amplification defects in nontransgenic cells (C339A, Y62A, T186Y, T186Y/E188Q, and 41-43-44) remained severely debilitated in the transgenic cells. Those mutants with moderate amplification defects (E188Q, 41-43, 41-44, and 43-44) maintained moderate amplification levels in each transgenic line. In the cases of the Y62A and 41-43 mutants, the NIa or 6/NIa lines, respectively, appeared to stimulate amplification modestly. However, stimulation was not observed with the CI/6/NIa lines. We were unable to demonstrate, therefore, that NIa functions could be supplied in *trans* by free NIa or by NIa derived from 6/NIa or CI/6/NIa polyproteins.

DISCUSSION

The NIa nuclear localization and VPg function. By using a reporter protein (GUS) fusion approach, the NIa sequence between positions 40 and 49 was shown to be sufficient for NLS activity. It is likely that this is the only NLS within the NIa protein, as all GUS/NIa fusion proteins lacking this sequence are unable to translocate to the nucleus. Because it contains a dense cluster of basic residues within a 10-amino-acid sequence, the NIa NLS likely belongs to the simian virus 40 large-T-antigen class of NLS (32). The presence of additional basic residues at positions 56 and 57 of NIa could be interpreted to indicate that residues 40 to 49 actually form part of a NLS belonging to the bipartite class (32), such as that within nucleoplasmin (37). However, as these residues are not required for NIa NLS activity, the position of these basic residues in relation to the 40–49 sequence may be fortuitous.

The GUS/NIa fusion proteins with substitutions affecting residues 41, 43, 44, and 48 localized in the cytoplasm, suggesting that these residues are critical for NLS function. Considering that three of these residues are either Lys or Arg, which are always clustered within the large T-antigen-type NLSs, this result was not surprising. However, the interpretation of these results was clouded by the finding that NIa proteins encoded by viruses containing single point mutations affecting these same residues were localized predominantly to the nucleus. Nuclear transport defects of NIa within virus-infected cells required combinations of at least two substitutions. In other words, transport of the transgenic fusion proteins was more sensitive to substitutions than was transport of authentic NIa in infected cells. This finding could indicate that nuclear transport of NIa is more efficient in virus-infected cells, possibly because of the presence of other viral factors. One such factor might be NIb, which is known to accumulate in equimolar ratios with NIa in the nuclei of infected cells (3, 4, 33). Alternatively, the structural integrity of NIa fused to GUS may be compromised compared with the structural integrity of nonfused NIa, rendering the fusion protein more sensitive to the single amino acid changes.

What is the role of nuclear translocation of NIa? While it is highly doubtful that any RNA replication events occur within the nucleus, transport of a proportion of NIa may be necessary for efficient genome amplification. The effects of mutations within the NLS coding region suggest a correlation between translocation activity and genome amplification levels. The single substitutions of K-41, K-43, and R-44 had only modest, if any, effects on NIa nuclear accumulation and also had relatively little effect on amplification. The double mutants affecting these positions had significant effects on both NIa nuclear transport and genome amplification. The degree of debilitation of amplification correlated with the extent of cytoplasmic accumulation. Those double mutants with the highest proportion of cells containing nuclear or partially nuclear/partially cytoplasmic localization (41-43 and 43-44) were amplified best, whereas the 41-44 mutant was amplified to the lowest level and encoded NIa that was predominately cytoplasmic. Two roles for translocation of NIa to the nucleus can be envisioned. First, NIa may interact with nuclear factors or structures to influence host functions, such as transcription. Pea seedborne mosaic potyvirus was shown to induce a transient inhibition of host mRNA accumulation in cells supporting virus replication (43). The basis for this inhibition is not known but could conceivably involve NIa within the nucleus. Second, transport of NIa to the nucleus could serve as a down-regulatory function for NIa activities in the cytoplasm. High concentrations of NIa in the cytoplasm could possibly be inhibitory to completion of the replicative cycle.

It should also be recognized that the amplification-debilitating effects of the NLS double and triple mutants could have been due to effects unrelated to NIa nuclear transport activity. Among the single NLS mutants, the K45A mutant was amplified to the lowest level, yet substitution of K-45 in the GUS/NIa fusion protein had no effect on nuclear transport. This finding suggests that the NLS overlaps other functional regions of NIa or that changes in the NLS affect other regions of the molecule. As the NLS is located 13 to 22 residues from Tyr-62, the RNA attachment site, there is a strong possibility that NLS changes affect VPg activity of NIa. In the absence of an in vitro assay for VPg function, it will be difficult to distinguish between effects due solely to changes in either NLS or VPg activity.

Internal cleavage of NIa. The internal cleavage site within NIa is utilized in a minority of NIa molecules within TEV-infected cells (13). Virtually all of the nuclear pool of NIa is full length, whereas the VPg pool linked to RNA is a mixture of full-length and internally processed forms. The slow-processing characteristic of this site is due, at least in part, to

residues in the P1 and P3 positions that deviate from the heptapeptide consensus sequence. Substitution of Glu-188 for Gln or Thr-186 for Tyr in the P1 or P3 position, respectively, converted this site to a consensus cleavage site and dramatically accelerated internal processing in vitro. These substitutions were detrimental to genome amplification, suggesting that the slow-processing feature at the internal site may serve an important regulatory function. The slow rate of processing would ensure a long half-life for full-length NIa and limited quantities of free VPg and proteinase domains. The slow cleavage activity may control the ratio between full-length and processed forms or may result in timed activation or deactivation of NIa functions. It is also possible that certain NIa functions involve the region of NIa spanning the internal cleavage site, in which case substitutions affecting the internal cleavage site could directly debilitate other activities.

While the full-length and internally processed forms of NIa are functional proteolytic enzymes (16), it is not clear in which forms NIa functions as VPg. The fact that the genome-linked pool of VPg contains both free VPg domain and full-length NIa could indicate that either form is functional. Alternatively, the processed form could arise from full-length NIa by internal processing after linkage to RNA. In either case, it was postulated that functional VPg involves a 6/NIa or 6/VPg polyprotein form (35). The 6-kDa protein functions as a membrane-binding protein that may anchor replication complexes to membrane-based sites of RNA replication. This model is similar to that proposed for picornaviruses in which the VPg (3B protein) is bound to a membrane via linkage with 3A protein within the 3AB polyprotein (19, 40).

Noncomplementation of NIa functions. Mutants with defects in several TEV-encoded proteins were shown previously to be rescued in transgenic plants expressing functional, individual proteins. Two classes of mutants with amplification defects, those with mutations affecting NIb polymerase or the accessory protein P1, can be complemented in transgenic cells expressing NIb or P1 protein, respectively (24, 41). Those data indicated clearly that at least some TEV RNA replication proteins are functional in *trans* when supplied outside the context of the viral polyprotein. In contrast, expression of NIa in transgenic cells was insufficient to rescue any of the NIa-defective mutants tested in this study.

The failure to complement the NIa mutants could have been due to one of several reasons. It is likely that some NIa functions require a polyprotein context. The proteinase, for example, exhibits a high preference for *cis* cleavage at certain sites in vitro (6, 8). The VPg activity, as stated above, is proposed to function within a polyprotein containing the 6-kDa protein, although neither cells expressing the 6/NIa polyprotein nor cells expressing the CI/6/NIa polyprotein were able to rescue the NIa-defective mutants. It is possible that the levels of NIa or NIa-containing polyproteins in the transgenic cells were insufficient to complement the defective viruses. The level of NIb required to rescue NIb-defective viruses in transgenic cells, however, is known to be lower than the levels of virus-encoded NIb synthesized in infected cells (24). It is possible that the CI/6/NIa polyprotein was processed too quickly in transgenic cells, thereby limiting the effective concentration of functional polyprotein, or that polyproteins larger than CI/6/NIa are required for delivery of NIa in a functional context. The lack of complementation could also have been the result of a requirement for coupling of translation and RNA replication. Novak and Kirkegaard (31) demonstrated that poliovirus RNA replication requires translation in *cis* through an internal region of the genome coding for several replication proteins. Weiland and Dreher (44) showed that replication of turnip yellow mosaic virus genomic RNA also requires translation through a sequence encoding a putative nucleoside triphosphate-binding protein. The molecular basis for coupling between translation and replication of genomic RNA is not clear but may involve a requirement for association of certain viral proteins with the RNA template from which they are encoded. If NIa functions involved in replication are *cis* preferential but NIb (polymerase) functions are not, this would imply that recruitment of TEV proteins into replication complexes can occur by distinct mechanisms.

ACKNOWLEDGMENTS

We thank Deon Freed, Kerri Herndon, Patricia Valdez, and Aaron Unterbrink for excellent technical assistance.

This research was supported by the National Institutes of Health (grants AI09121 to M.C.S. and AI27832 to J.C.C.) and the U.S. Department of Agriculture (grant NRICG 95-37303-1867).

REFERENCES

1. **Allaire, M., M. M. Chernaia, B. A. Malcolm, and M. N. James.** 1994. Picornaviral 3C cysteine proteinases have a fold similar to chymotrypsin-like serine proteinases. Nature (London) **369:**72–76.
2. **An, G.** 1986. Development of plant promoter expression vectors and their use for analysis of differential activity of nopaline synthase promoter in transformed tobacco cells. Plant Physiol. **81:**86–91.
3. **Baunoch, D., P. Das, and V. Hari.** 1988. Intracellular localization of TEV capsid and inclusion proteins by immunogold labeling. J. Ultrastruc. Mol. Struct. Res. **99:**203–212.
4. **Baunoch, D. A., P. Das, M. E. Browning, and V. Hari.** 1991. A temporal study of the expression of the capsid, cytoplasmic inclusion and nuclear inclusion proteins of tobacco etch potyvirus in infected plants. J. Gen. Virol. **72:**487–492.
5. **Bazan, J. F., and R. J. Fletterick.** 1988. Viral cysteine proteases are homologous to the trypsin-like family of serine proteases: structural and functional implications. Proc. Natl. Acad. Sci. USA **85:**7872–7876.
6. **Carrington, J. C., S. M. Cary, and W. G. Dougherty.** 1988. Mutational analysis of tobacco etch virus polyprotein processing: *cis* and *trans* proteolytic activities of polyproteins containing the 49-kilodalton proteinase. J. Virol. **62:**2313–2320.
7. **Carrington, J. C., S. M. Cary, T. D. Parks, and W. G. Dougherty.** 1989. A second proteinase encoded by a plant potyvirus genome. EMBO J. **8:**365–370.
8. **Carrington, J. C., and W. G. Dougherty.** 1987. Processing of the tobacco etch virus 49K protease requires autoproteolysis. Virology **160:**355–362.
9. **Carrington, J. C., and W. G. Dougherty.** 1987. Small nuclear inclusion protein encoded by a plant potyvirus genome is a protease. J. Virol. **61:**2540–2548.
10. **Carrington, J. C., and D. D. Freed.** 1990. Cap-independent enhancement of translation by a plant potyvirus 5′ nontranslated region. J. Virol. **64:**1590–1597.
11. **Carrington, J. C., D. D. Freed, and A. J. Leinicke.** 1991. Bipartite signal sequence mediates nuclear translocation of the plant potyviral NIa protein. Plant Cell **3:**953–962.
12. **Carrington, J. C., D. D. Freed, and C.-S. Oh.** 1990. Expression of potyviral polyproteins in transgenic plants reveals three proteolytic activities required for complete processing. EMBO J. **9:**1347–1353.
13. **Carrington, J. C., R. Haldeman, V. V. Dolja, and M. A. Restrepo-Hartwig.** 1993. Internal cleavage and *trans*-proteolytic activities of the VPg-proteinase (NIa) of tobacco etch potyvirus in vivo. J. Virol. **67:**6995–7000.
14. **Dolja, V. V., H. J. McBride, and J. C. Carrington.** 1992. Tagging of plant potyvirus replication and movement by insertion of β-glucuronidase into the viral polyprotein. Proc. Natl. Acad. Sci. USA **89:**10208–10212.
15. **Dougherty, W. G., S. M. Cary, and T. D. Parks.** 1989. Molecular genetic analysis of a plant virus polyprotein cleavage site: a model. Virology **171:**356–364.
16. **Dougherty, W. G., and T. D. Parks.** 1991. Post-translational processing of the tobacco etch virus 49-kDa small nuclear inclusion polyprotein: Identification of an internal cleavage site and delimitation of VPg and proteinase domains. Virology **183:**449–456.
17. **Dougherty, W. G., and B. L. Semler.** 1993. Expression of virus-encoded proteinases: functional and structural similarities with cellular enzymes. Microbiol. Rev. **57:**781–822.
18. **García, J. A., J. L. Riechmann, and S. Laín.** 1989. Proteolytic activity of the plum pox potyvirus NIa-like protein in *Escherichia coli*. Virology **170:**362–369.
19. **Giachetti, C., and B. L. Semler.** 1991. Role of a viral membrane polypeptide in strand-specific initiation of poliovirus RNA synthesis. J. Virol. **65:**2647–2654.

20. **Gorbalenya, A. E., A. P. Donchenko, V. M. Binov, and E. V. Koonin.** 1989. Cysteine proteases of positive strand RNA viruses and chymotrypsin-like serine proteases. FEBS Lett. **243:**103–114.
21. **Hellmann, G. M., J. G. Shaw, and R. E. Rhoads.** 1988. *In vitro* analysis of tobacco vein mottling virus NIa cistron: evidence for a virus-encoded protease. Virology **163:**554–562.
22. **Jefferson, R. A.** 1987. Assaying chimeric genes in plants: the GUS gene fusion system. Plant Mol. Biol. Rep. **5:**387–405.
23. **Li, X. H., and J. C. Carrington.** 1993. Nuclear transport of tobacco etch potyviral RNA-dependent RNA polymerase is highly sensitive to sequence alterations. Virology **193:**951–958.
24. **Li, X. H., and J. C. Carrington.** 1995. Complementation of tobacco etch potyvirus mutants by active RNA polymerase expressed in transgenic cells. Proc. Natl. Acad. Sci. USA **92:**457–461.
25. **Martín, M. T., and J. A. García.** 1991. Plum pox potyvirus RNA replication in a crude membrane fraction from infected *Nicotiana clevelandii* leaves. J. Gen. Virol. **72:**785–790.
26. **Matthews, D. A., W. W. Smith, R. A. Ferre, B. Condon, G. Budahazi, W. Sisson, J. E. Villafranca, C. A. Janson, H. E. McElroy, C. L. Gribskov, and S. Worland.** 1994. Structure of human rhinovirus 3C protease reveals a trypsin-like polypeptide fold, RNA-binding site, and a means for cleaving precursor polyprotein. Cell **77:**761–771.
27. **Matthews, R. E. F.** 1991. Plant virology. Academic Press, Inc., San Diego, Calif.
28. **Murphy, J. F., R. E. Rhoads, A. G. Hunt, and J. G. Shaw.** 1990. The VPg of tobacco etch virus RNA is the 49 kDa proteinase or the N-terminal 24 kDa part of the proteinase. Virology **178:**285–288.
29. **Murphy, J. F., W. Rychlik, R. E. Rhoads, A. G. Hunt, and J. G. Shaw.** 1990. A tyrosine residue in the small nuclear inclusion protein of tobacco vein mottling virus links the VPg to the viral RNA. J. Virol. **65:**511–513.
30. **Negrutiu, I., R. Shillito, I. Potrykus, G. Biasini, and F. Sala.** 1987. Hybrid genes in the analysis of transformation conditions. 1. Setting up a simple method for direct gene transfer in plant protoplasts. Plant Mol. Biol. **8:**363–373.
31. **Novak, J. E., and K. Kirkegaard.** 1994. Coupling between genome translation and replication in an RNA virus. Genes Dev. **8:**1726–1737.
32. **Raikhel, N. V.** 1992. Nuclear targeting in plants. Plant Physiol. **100:**1627–1632.
33. **Restrepo, M. A., D. D. Freed, and J. C. Carrington.** 1990. Nuclear transport of plant potyviral proteins. Plant Cell **2:**987–998.
34. **Restrepo-Hartwig, M. A., and J. C. Carrington.** 1992. Regulation of nuclear transport of a plant potyvirus protein by autoproteolysis. J. Virol. **66:**5662–5666.
35. **Restrepo-Hartwig, M. A., and J. C. Carrington.** 1994. The tobacco etch potyvirus 6-kilodalton protein is membrane-associated and involved in viral replication. J. Virol. **68:**2388–2397.
36. **Riechmann, J. L., S. Laín, and J. A. García.** 1992. Highlights and prospects of potyvirus molecular biology. J. Gen. Virol. **73:**1–16.
37. **Robbins, J., S. M. Dilworth, R. A. Laskey, and C. Dingwall.** 1991. Two interdependent basic domains in nucleoplasmin nuclear targeting sequence: identification of a class of bipartite nuclear targeting sequence. Cell **64:**615–623.
38. **Shahabuddin, M., J. G. Shaw, and R. E. Rhoads.** 1988. Mapping of the tobacco vein mottling virus VPg cistron. Virology **163:**635–637.
39. **Slade, D. E., R. E. Johnston, and W. G. Dougherty.** 1989. Generation and characterization of monoclonal antibodies reactive with the 49-kDa proteinase of tobacco etch virus. Virology **173:**499–508.
40. **Takegami, T., B. L. Semler, C. W. Anderson, and E. Wimmer.** 1983. Membrane fractions active in poliovirus RNA replication contain VPg precursor polypeptides. Virology **128:**33–47.
41. **Verchot, J., and J. C. Carrington.** 1995. Evidence that the potyvirus P1 protein functions as an accessory factor for genome amplification. J. Virol. **69:**3668–3674.
42. **Verchot, J., E. V. Koonin, and J. C. Carrington.** 1991. The 35-kDa protein from the N-terminus of a potyviral polyprotein functions as a third virus-encoded proteinase. Virology **185:**527–535.
43. **Wang, D., and A. J. Maule.** 1995. Inhibition of host gene expression associated with plant virus replication. Science **267:**229–231.
44. **Weiland, J. J., and T. W. Dreher.** 1993. cis-preferential replication of the turnip yellow mosaic virus RNA genome. Proc. Natl. Acad. Sci. USA **90:**6095–6099.